

A 44-year (1958-2001) sea level residual hindcast over the Mediterranean Basin within the HIPOCAS Project framework

Ratsimandresy, A.W.^{*†}, M.G. Sotillo[†], E. Álvarez Fanjul[†], J.C. Carretero Albiach[†], B. Pérez Gómez[†], H. Hajji[‡]

[†] Ente Público Puertos del Estado, Madrid, Spain

^{*}NAFC, Fisheries and Ocean Canada, St. John's, NL, Canada

[‡]Meteomer, France. Present address: GlobOcean Sarl, France

Corresponding address: *ratsimandresya@dfo-mpo.gc.ca*

A 44-year (1958-2001) sea level residual hindcast over the Mediterranean Basin within the HIPOCAS Project framework

Ratsimandresy, A.W.*† M. G. Sotillo† E. Álvarez Fanjul†
J.C. Carretero Albiach† B. Pérez Gómez† H. Hajji‡

Abstract

The present work describes a 44-year integration of a sea level model over the Mediterranean Sea performed within the framework of the HIPOCAS European Project. As an output of such long-term hindcast a sea surface residual database containing storm surge events was configured. Sea level is a very important variable that must be used in combination with wave parameters in order to properly describe the sea status. Storm surge is a critical parameter in different kinds of studies, from harbour design to coastal dynamics. Since the climatic trends of total sea surface elevation depends very much on global processes making it too far beyond the scope of this research project, this work is focused on studying the regional evolution of the contribution of the atmospheric forcing on the residual sea surface variation. The modeling of sea level residual is of particular interest in the Mediterranean Sea because the tide amplitude is very low whereas the response of the sea to the atmospheric forcing can be a significant signal. The integration was performed by means of the HAMSOM numerical model. It is a three-dimensional, z-coordinate, finite difference model in Arakawa C grid. In the present research, the model was used in its barotropic version by integrating vertically the primitive equations. Hourly HIPOCAS hindcasted wind and atmospheric sea level pressure fields were used to force the sea level model. These forcing fields were generated by dynamical downscaling from the NCEP/NCAR global reanalysis through the atmospheric REMO model. Main results of the work including trends of mean residual sea surface as well as that of the extreme events are reported and analyzed.

*Present address: NAFC, Fisheries and Ocean Canada, St. John's, NL, Canada

†Ente Público Puertos del Estado, Madrid, Spain

‡Meteomer, France. Present address: GloOcean Sarl, France

1 Introduction

Nowadays, there is an increase in the need of long term oceanographic and atmospheric databases for wide applications such as offshore industries, fisheries, shipping companies, insurance businesses, and tourism. With respect to sea level, the necessity of understanding its variation has been growing. This is because sea level rises have been reported to take place globally (as reported by Church *et al.* 2001, Cazenave *et al.* 1998, Cabanes *et al.* 2001, and much more) and in regions like the Mediterranean Sea (Ross *et al.* 2000, Shriman and Mezier 2002, Cazenave *et al.* 2001, to name but a few) or others (Joyce and Robbins 1996, and Bindoff and McDougall 2000 for example).

The rise in sea level is the result of various processes including global warming which leads to ice melting and ocean water expansion due to deep and surface ocean warming, vertical movement of land, change in atmospheric forcing, and change in river runoff into the ocean. The contribution of each process varies depending on the region. For instance, Schönwiese and Rapp and Schönwiese *et al.* found a sea level change change of -0.05 and $+0.04$ mm/yr between 1960 and 1990 as a result of regional changes in surface pressure.

The EU-funded research project “Hindcast of Dynamic Processes of the Ocean and Coastal Areas of Europe (HIPOCAS)” is partly fulfilling that need of long-term environmental datasets by generating more than four decades of atmospheric and oceanographic databases. These hindcasted datasets include numerous atmospheric variables at different levels, as well as residual sea surface (hereafter RSS) and wave fields for European waters.

This work analyzes the result obtained by the Spanish harbor office (*Ente Público Puertos del Estado*, EPPE) for their contribution to the HIPOCAS project with respect to sea-level. It is organized in the following way: the model setup is briefly described in Section 2, the sea level data together with its comparison with in-situ measurements is presented in Section 3, the general long term statistics for the entire Mediterranean Basin is analyzed in Section 4, and the climatological analysis of the hindcast data is examined in Section 5 followed by discussions about the result (Section 6) and the conclusion.

2 Models Set-up

The RSS data had been generated with the HAMSOM (HAMBurg Shelf Ocean Model) numerical model (Backhaus 1983). The version of the numerical model used was similar to that used by EPPE for its operational storm surge forecast system (Álvarez Fanjul 1998). It was developed within their collaboration with the Institut für Meerskunden, Hamburg, Germany (Rodríguez and Álvarez 1991, Rodríguez *et al.* 1991, Álvarez-Fanjul *et al.* 1997) for an operational application. It is presently used in the barotropic mode for routinely computing the 6-hourly RSS in the

Mediterranean Basin. HAMSOM is a circulation model based on the ocean primitive equations which follow the hydrostatic approximation with a free surface. Spatial grids are defined on the Arakawa-C grid following Z-coordinates in the vertical. In the model integration, the pressure gradient and the vertical diffusivity terms are integrated using a semi-implicit scheme while the momentum advection and the horizontal diffusion using an explicit one. No tidal forcing was included in the performed hindcast because non-linear interactions of this forcing with residuals over the simulation domain are weak, and thus neglectable (Álvarez Fanjul 1998).

The model domain covers the whole Mediterranean Basin as well as part of the northeastern Atlantic Ocean (Figure 1). The zonal boundaries are set at 30°N in the south and at 46°N in the north, whereas the longitudinal ones are at 14°W, and at 36°E. The Black Sea is not studied by setting its depth to the land mask value. No fresh water runoff and no water exchange between basins are included, apart from the Strait of Gibraltar which lies within the domain. The grid resolution is uniform for the whole domain: 15' by 10' in longitude and latitude, respectively. This choice of resolution was made after testing a higher one (10' by 6' in longitude and latitude, respectively) which turns out to unreasonably increase the necessary computer resources without bringing a noticeable improvement in the result. The HAMSOM model is forced with hourly hindcasted mean sea level pressure and 10-m wind fields. As part of the HIPOCAS project, this atmospheric forcing was produced by a dynamical downscaling of the NCEP/NCAR reanalysis using the REgional MOdel, REMO. A detailed description of this Mediterranean atmospheric HIPOCAS hindcast, as well as its validation, is presented in the work of Sotillo *et al.* (2005). This atmospheric hindcast was performed for a 44-year period, from January 1958 to December 2001, with hourly outputs over the whole Mediterranean Basin.

[Figure 1 about here.]

3 Data

The 44-year hindcasted RSS data is currently part of a long term oceanographic and atmospheric database maintained by PE. Before including the HIPOCAS hindcast RSS data within the database, an exhaustive validation study has been carried out in order to assess its quality. Such validation consisted on comparing time series from various in-situ measurements with those obtained from the simulation. In this study, we show the comparison of time series of residuals from nine different tide gauges located along the Spanish coast. These tide gauges belong to the PE REDMAR network (Pérez and Rodríguez 1994). As can be seen in Figure 1, three of them located in the Mediterranean (BARC, VALE, MALG), four along the northern coast of the Iberian Peninsula (BILB, SANT, GIJO, CORU), one on the western coast (VIGO), and a last one in the southern part of Spain (HUEL). In-situ residuals were obtained by first removing the tidal com-

ponents. These components were computed by means of the Foreman Analysis and Prediction programs (Foreman 1977). In order to compare the hindcasted RSS with in-situ data, model data were extracted from the closest grid point to each station. Both sets of data are available with an hourly time interval. In total, for the whole 9 series, some 69 years of hourly data were available for the validation of the model result.

Fig. 2 shows the comparison of 4-month measurements with simulated residuals from the tide gauge at the Barcelona harbour. One can observe that the model is able to simulate accurately the observed temporal evolution of the residuals. Few underestimations are also found. Nonetheless, the index of correlation between the two sets of series is relatively high as summarized in the Table 1. An index of between 0.71 (for station at Málaga harbor, MALG) and 0.88 (for station at Vigo, VIGO) is obtained. With respect to the root mean square (rmse) it ranges from 5.26 to 6.60 with the highest error found at HUEL and the lowest at BARC. The error found at HUEL might be attributed to the location of the tide gauge. It is also worth to point out that filtering away from the series the high and low frequencies, not related to the meteorological effects, the correlation indexes increase notably their values.

[Figure 2 about here.]

[Table 1 about here.]

Fig. 3 illustrates the geographic distribution of the time correlations. According to the skills of the hindcast data to reproduce the in-situ measurements representing by the correlation values, three groups can be splitted, namely the region where the index of correlation is higher than 0.84, the region where it is between 0.75 and 0.84, and finally the area where the index is lower than 0.75. The first group includes the tide gauges along the northwestern and northern coast of Spain, namely BILB, SANT, GIJO, CORU, and VIGO. The second group is composed of the Mediterranean tide gauges located along the eastern Spanish coast (BARC and VALE). And the last group includes the gauges located south of the Iberian Peninsula, on both sides of the Strait of Gibraltar (HUEL and MALG). Note that the lower agreement for these two southern stations may be justified for the location of the tide gauge. In the case of HUEL, the tide gauge is located close to a river mouth with the consequently changes in the sea level, specially during strong precipitation events. On the other hand, MALG tide gauge is located in an area highly affected by baroclinic effects.

[Figure 3 about here.]

With respect to RSS longer term variations, Fig. 4 shows a comparison of monthly mean RSS from the tide gauge located at VIGO for a period of 9 years. One can observe a fairly good correspondence between the time series although an underestimation is found at the beginning of

1996 or at mid-2001. Such failure is attributed to a tendency of the model to underestimate very large surges. This shortcoming can be observed at various strong storm events and is also found at some other locations where the in-situ measurements are available (Figures not shown).

[Figure 4 about here.]

In order to complete the validation, the hindcasted residuals have also been compared with data inferred from remote sensing measurements. For that, residual sea surface was extracted from the Topex/Poseidon altimeter data at the location closest to the position of the tide gauge. Figure 5 illustrates such comparison at the BARC station. Some statistics for this case as well as for other locations are provided in Table 2. For all the cases, but MALG, the correlation between the satellite and the simulation data is relatively high (over 0.74) reinforcing the idea that the hindcast RSS can be considered as representing the RSS around the Iberian Peninsula, and as an extrapolation over the Mediterranean Basin in general.

[Figure 5 about here.]

[Table 2 about here.]

This high quality of the data is also confirmed by some indirect analysis (García Lafuente *et al.* 2002) where the integrated flow through the Strait of Gibraltar was compared with the transport computed by early studies. In their analysis, García Lafuente *et al.* have shown that the transport from the HIPOCAS data gives better correlation with the in-situ measurements when the model is forced by atmospheric pressure together with the wind stress. They also emphasize on the importance of the wind forcing as it improves the simulation in comparison to the atmospheric-only forced model case.

4 Long term statistics of the RSS over the Mediterranean Basin

In this section, the main features derived from the HIPOCAS RSS long term statistics as well as its different regional spatial distribution are described.

As illustrated in figure 6, the map of mean RSS over the entire basin shows an interesting feature. First of all, it slopes upward from the west to the east. The highest mean residual level is found at the very eastern part of the Basin with a value of 8.5 cm, while the lowest, east of the Strait of Gibraltar reaches values around 1.8 cm. On the western side of the Strait, the mean residual sea level is lower, with a minimum found along the western African and Iberian coasts. This characteristic might be attributed to the existence of strong upwelling along these coasts

(Nykjaer and Van Camp 1994) although this upwelling undergoes seasonal variation. The mean RSS field shows a coincident pattern with the long term mean sea level pressure field derived from the atmospheric HIPOCAS hindcast (Figure 7), giving an important role to the inverted barometer effect on the long term residual sea level. The standard deviation (Figure not shown) presents some features such that a deviation as high as 14 cm is found in the Adriatic Sea, and as low as 3 - 4 cm off the Atlantic African coast. For the Mediterranean Basin, the lowest deviation, between 5 and 6 cm, is observed in the south-east part, offshore of the Libyan and the Egyptian coast. Off the Spanish Mediterranean coast, the deviation is increasing from the south to the north with values ranging between 6 and 9 cm.

[Figure 6 about here.]

[Figure 7 about here.]

With respect to minimum RSS at each grid location (Figure not shown), the range of values is of the order of 110 cm with the lowest minimum (approximately 120 cm below the reference) observed in the northern part of the Adriatic Sea. The map of maximum RSS shows that the highest maximum is also found in the north Adriatic Sea with a level of more than 140 cm (Fig. 8). The map of maximum RSS reveals that, the southern regions of the Mediterranean show lower maximum level in comparison with the northern ones. This latitudinal gradient in the maxima is in contrast with the map of mean RSS or minimum RSS, where not any special latitudinal gradient are observed over the Basin. More specifically, around the Spanish Mediterranean coast, the maximum RSS is approximately 40 cm. The range of maximum values for the entire domain is over 130 cm with the lowest maximum observed in the southwest domain, in the Atlantic.

[Figure 8 about here.]

5 Climatology of the RSS over the Mediterranean Basin

As part of the objectives of the present study, it is of main importance to assess the RSS climatology of the Mediterranean Basin. The HIPOCAS hindcasted RSS data can be very useful to reach this objective as it covers the entire basin and is available at high frequency (hourly) for a period of more than four decades.

First, we should mention that the atmospheric fields used to force the circulation model have been extensively validated (Sotillo 2003, Sotillo *et al.* 2005). Such validation was performed by doing a direct comparison of the surface parameters such as temperature, wind velocity, and pressure with measurements and remote sensed data. Special attention was paid on verifying the homogeneity of the atmospheric fields. Sotillo (2003) verified that the atmospheric HIPOCAS

hindcasted fields do not present any kind of inhomogeneity or spurious trends. Taking into account that the HAMSOM model is kept identical along the whole 44-year hindcast period, as well as the fact that over this period the atmospheric forcing is homogeneous, one can consider the resulting hindcasted RSS output will be also pretty homogeneous and therefore an useful tool to carry out long term climatological studies over the Mediterranean Basin.

A statistical analysis of the variability and long term trends in RSS means and for different RSS percentile levels were carried out at each grid point. This analysis was performed on annual basis, being the trends then calculated at each grid point as simple linear trends over the 44 yearly values. Fig. 9 illustrates an example of such calculations for a grid point located in the Gulf of Lyon (4.0E, 42.5N). In this figure, seven percentile levels are presented, namely, the maximum (100th percentile), the 99th percentile, and the 90th percentile, together with their symmetry in the minimum part (10th percentile, 1st percentile, and minimum or 0th percentile) as well as the 50th percentile. For this specific grid, one can observe that all the percentiles show negative trends during the 44 years of hindcast. The yearly RSS maxima have undergone a decrease of approximately 6 cm over the 44 years giving a change of -1.36 mm/y. For the mean regime (here given by the 50th percentile), the change is also negative but with a lesser range of the order of 2 cm over the 44 years. Therefore, the mean RSS at this location is lowering at a rate of 0.45 mm/y.

[Figure 9 about here.]

Fig. 10a illustrates the geographical distribution of of RSS change rates for the whole domain. The maximum decreasing rate (of the order of -0.7 mm/y) is found in the central Mediterranean Basin (including the northern Adriatic) and the northeastern part of the Basin, north of Cyprus. For the Spanish Mediterranean region, the RSS is also dropping but with a lower rate (approximately -0.5 mm/y). In the Atlantic, the rate is lower than in the Mediterranean Basin. The lowest change rates (-0.3 mm/y) are found over the open Atlantic Ocean and along the western Iberian and North African coasts.

When looking at the RSS extreme values characterized by percentile 99th (Fig. 10b), the overall trends for the entire domain is a drop with rates as high as -2.00 mm/yr. Regional differences are observed. The highest drop is found in the northern Adriatic area and the lowest in the Ionian region (east of Sicily) with a rate between -0.50 and -0.25 mm/yr. Off the Iberian Peninsula, the rate of drop ranges between -1.00 and -0.75 mm/yr except along the northwestern coast where the rate is larger than -1.00 mm/yr. These trends are significance at 90% level for most of the areas of the basin.

[Figure 10 about here.]

6 Discussion

Whereas the hindcasted RSS compares well in general terms with in-situ measurements, the model shows some difficulties in efficiently simulate very strong storms. This failure might be explained by some underestimation of the wind fields used to force the circulation model. This underestimation is indirectly observed using a wave model which is forced by the same wind fields. Such experiments were part of the present project (Guedes Soares *et al.* 2002, Ratsimandresy and Sotillo 2003). The hindcast of waves in the western Mediterranean has shown that due to an underestimation of the westerly winds (*poniente* events), the measured significant wave heights in the Alboran Sea tend to be undervalued by the hindcast waves. Such shortage takes place in most of the regions where the wind is blowing offshorewards through an abrupt orography change from land to ocean. Despite of this shortcoming the HIPOCAS datasets can be seen currently as one of the best available tool to characterize the Mediterranean RSS climate.

It can be seen that around the Iberian Peninsula, where a more exhaustive HIPOCAS hindcast validation has been performed, and more specifically along its North and Northwestern coasts marked by mainly shoreward winds, the atmospheric state is better reproduced than along its Mediterranean coasts. This different skill in reproducing the prevailing wind conditions is determinant to explain the existence of regional difference in the simulation of the RSS hindcast data. In that sense, it is expected (and has been confirmed) that over the Atlantic the hindcasted data better correlates with the in-situ observations than over the Mediterranean or around the Strait of Gibraltar since the wind fields are more realistic in the Atlantic than along the Spanish Mediterranean coast. This is in accordance with Carretero *et al.* (2000) who highlighted the need of good wind forcing to improve the correlation between model and observation data.

In this study the residual sea surface is constituted mainly by the inverted barometer and partially by the wind effects. The hindcast was performed with a numerical model set-up that not allow to include any heat exchange between the atmosphere and the ocean, nor did it consider the steric variability due to the variation of temperature of the ocean. Therefore, any long term variability and trends shown by the RSS will reflect similar change in the atmospheric pressure and wind fields in the area. In this sense and with respect to the long term variation of sea surface, the result obtained with the HIPOCAS data over the Mediterranean Basin is concurrent with the increase in atmospheric pressure stated by Tsimplis and Josey (2001). Their assessment is based on the Permanent Service for Mean Sea Level database (Spencer and Woodworth, 1993) which covers a 34 years period (between 1960 and 1994). According to Tsimplis and Rixen (2002) the 1.3 mm/y sea level drop reported by Tsimplis and Baker (2000) for the period after 1960 should have some inverse barometer components. The present study is showing that in the central areas of the Mediterranean Basin, almost half part of such components can be explained by the meteorological forcing consisting of the barometric and the wind stresses effects. In the western

Mediterranean, the role of the meteorological forcing in the sea level trends is weaker and some other processes should be considered to explain the observation.

In contrast with the other processes such as the changes in the exchange flow through the Strait of Gibraltar (Ross *et al.* 2000) and the expansion of the ocean due to increase of temperature (Tsimplis and Rixen 2002, Cazenave *et al.* 2001) to which a rise of sea level is attributed, the atmospheric response of the sea level has been responsible of a drop for the second half part of the twentieth century.

7 Conclusions

44 years of sea surface residuals have been generated by means of the HAMSOM numerical model driven by the HIPOCAS hindcasted atmospheric forcing. Both hindcasts were carried out within the HIPOCAS research project with the objectives of completing and improving atmospheric and oceanographic databases for Mediterranean waters and off the Atlantic European coast. The hindcasted RSS is available every hour with a high spatial resolution of approximately 21 km by 17 km in longitude and latitude, respectively.

To the authors' knowledge, this work is one of the first temptatives to carry out a long term study of RSS in the Mediterranean with a relatively high resolution. It is of great interest the fact that the long term mean residual sea surface responds pretty well to the mean sea level pressure over the Mediterranean. While it confirms the main driving force for the sea surface height in the Mediterranean, one needs to also have available a good wind forcing as the later is necessary to improve the skills of the simulation to reproduce very high storm events.

The data generated in the present study has shown to agree well with the residuals computed from in-situ measurements. As such, it can be used as a helpful tool to verify and to make quality control of some observation series, especially when these present some kind of inhomogeneities due to instrumentation failure, or instruments and/or reference changes. This kind of problems is quite common with data obtained from old instruments or when updates to new method or instrumentation were made.

The climatologic study of the RSS has shown that its long term mean RSS values are higher on the western Mediterranean than over the eastern part. In the Atlantic RSS is even lower with an upwelling signature (low mean RSS) along the coast. With respect to the long term trends, the mean RSS for the whole basin shown a drop along the 44-year period (from 1958 to 2001) with a maximum change rate located over the central part of the basin. In the Atlantic, it has also dropped but with a lower rate. Although, with a lower order of magnitude than the sea level rise reported by previous studies for the Mediterranean Basin (Cazenave *et al.* 2001, Tsimplis and Rixen 2002) it should be taken into account when computing the variation of the sea level as it will give some correction on the role of each process in rising or dropping the level.

Acknowledgements

The “Hindcast of Dynamic Processes of the Ocean and Coastal Areas of Europe (HIPOCAS)” is a research project funded by the European Union under the Program “Energy, Environment and Sustainable Development” (Contract No EVK2-CT-1999-00038). In the project, EPPE has been responsible for the implementation and carrying out the atmospheric and oceanographic (sea-level and waves) hindcast for the Mediterranean and is also maintaining a public atmospheric and oceanographic database which includes the hindcasted data (<http://www.puertos.es/>). The in-situ data is part of the operational REDMAR network maintained by EPPE.

References

- [1] Álvarez Fanjul, E. *Simulación numérica de procesos oceanográficos en las Costas Atlánticas Españolas*. PhD dissertation, Universidad de Alcalá, 1998.
- [2] Álvarez-Fanjul, E., B. Pérez Gómez, and I. Rodríguez Sánchez-Arévalo. A description of the tides in the eastern North Atlantic. *Progress in Oceanography*, 40:217–244, 1997.
- [3] Backhaus, J. O. A semi-implicit scheme for the shallow water equations for application to shelf sea modelling. *Continental Shelf Res.*, 2:243–254, 1983.
- [4] Bindoff, N.L. and T.J. McDougall. Decadal changes along an Indian Ocean section at 32s and their interpretation. *Journal of Physical Oceanography*, 30(6):1207–1222, 2000.
- [5] Cabanes, C., A. Cazenave, and C. Le Provost. Sea level rise during past 40 years determined from satellite and in situ observations. *Science*, 294:840–842, 2001.
- [6] Carretero-Albiach, J.C., E. Álvarez-Fanjul, M. Gómez-Lahoz, B. Pérez-Gómez, and I. Rodríguez Sánchez-Arévalo. Ocean forecasting in narrow shelf seas: Application to the Spanish coasts. *Coastal Engineering*, 41:269–293, 2000.
- [7] Cazenave, A., C. Cabanes, K. Dominh, and S. Mangiarotti. Recent sea level change in the Mediterranean Sea revealed by Topex/Poseidon satellite altimetry. *Geophysical Research Letters*, 28:1607–1610, 2001.
- [8] Cazenave, A., K. Dominh, M.C. Gennero, and B. Ferret. Global mean sea level changes observed by Topex/Poseidon and ERS-1. *Phys. Chem. Earth*, 23:1069–1075, 1998.
- [9] Church, J.A., J.M. Gregory, P. Huybrechts, M. Kuhn, K. Lambeck, M.T. Nhuan, D. Qin, P.L. Woodworth, and all. *Changes in sea level*, chapter 11, pages 639–693. Intergovernmental Panel on Climate Change, 2001.
- [10] Foreman, M.G.G. *Manual for Tidal Heights Analysis and Prediction*. Institute of Ocean Sciences, Patricia Bay, Sidney, B.C. Canada, 1977. Pacific Marine Science Report 77-10.

- [11] García-Lafuente, J., E. Álvarez Fanjul, J.M. Vargas, and A.W. Ratsimandresy. Subinertial variability in the flow through the strait of gibraltar. *Journal of Geophysical Research*, 107:3168, doi:10.1029/2001JC001104, 2002.
- [12] Guedes Soares, C., J.C. Carretero, R. Weisse, and E. Álvarez. A 40 years hindcast of wind, sea level and waves in European waters. In *Proceedings of OMAE 2002, 21th International Conference on Offshore Mechanics and Artic Engineering*, page 7 pp., Oslo, Norway, June 2002.
- [13] Joyce, T.M. and P. Robbins. The long-term hydrographic record at bermuda. *Journal of Meteorology*, 9:3121–3131, 1996.
- [14] Nykjaer L. and L. Van Camp. Seasonal and interannual variability of coastal upwelling along northwest Africa and Portugal form 1981 to 1991. *Journal of Geophysical Research*, 99:14197–14207, 1994.
- [15] Pérez Gómez, B. and I. Rodríguez Sánchez-Arévalo. Redmar. Spanish harbour tidal gauge network. Processing of tidal data. Technical Report 57, Clima Marítimo, Madrid, Spain, 1994.
- [16] Ratsimandresy, A.W. and M.G. Sotillo. Reanálisis de 44 años (1958-2001) del clima oceánico y atmosférico en el Mar Mediterráneo: Informe técnico de la contribución de Puertos del Estado al proyecto europeo HIPOCAS. Technical report, Ente Público Puertos del Estado, Madrid, Spain, October 2003.
- [17] Rodríguez, I. and E. Álvarez Fanjul. Modelo tridimensional de corrientes. Condiciones de aplicación a las costas Españolas y análisis de resultados para el caso de un esquema de mallas anidadas. Technical Report 42, Programa de Clima Marítimo, Madrid, 1991.
- [18] Rodríguez, I., E. Álvarez Fanjul, J. Krohn, and J. Backhaus. A mid-scale tidal analysis of waters around the north-western corner of the Iberian Peninsula. In *9th Computer modelling in Ocean Engineering*, Balkema, 1991.
- [19] Ross, T., C. Garrett, and P.-Y. Le Traon. Western Mediterranean sea-level rise: changing exchange flow through the Strait of Gibraltar. *Geophysical Research Letters*, 27:2949–2952, 2000.
- [20] Schönwiese, C.-D. and J. Rapp. *Climate trends atlas of Europe based on observation*. Kluwer Academic Publisher, Dordrecht, 1997.
- [21] Schönwiese, C.-D., J. Rapp, T. Fuchs, and M. Denhard. Observed climate trends in europe 1891-1990. *Meteorol. Zeitschrift*, 3:22–28, 1994.
- [22] Shirman, B. and Y. Melzer. Mediterranean sea level changes over the period 1961–2000. In *XXII FIG International Congres*, page 11 pp., Washington, DC, USA, 2002.

- [23] Sotillo, M.G. *High-resolution multi-decadal atmospheric reanalysis in the Mediterranean Basin*. PhD thesis, Universidad Complutense de Madrid, Madrid, September 2003.
- [24] Sotillo, M.G., A.W. Ratsimandresy, J.C. Carretero, A. Bentamy, F. Valero, and F. González-Rouco. A high-resolution 44-year atmospheric hindcast for the Mediterranean Basin: Contribution to the regional improvement of global reanalysis. Submitted to *Clim. Dynam.*, 2005.
- [25] Spencer, N.E. and P.L. Woodworth. Data holdings of the Permanent Service of Mean Sea Level (November 1993). Technical report, Bidston, Permanent Service for Mean Sea Level, Birkenhead, 1993.
- [26] Tsimplis, M.N. and T.F. Baker. Sea level drop in the Mediterranean Sea: An indicator of deep water salinity and temperature changes? *Geophysical Research Letters*, 27:1731–1734, 2000.
- [27] Tsimplis, M.N. and S.A. Josey. Forcing of the Mediterranean Sea by atmospheric oscillations over the North Atlantic. *Geophysical Research Letters*, 28:803–806, 2001.
- [28] Tsimplis, M.N. and M. Rixen. Sea level in the Mediterranean Sea: The contribution of temperature and salinity changes. *Geophysical Research Letters*, 29:2136,doi:10.1029/2002GL015870, 2002.

List of Figures

1	Spatial domain covered by the HIPOCAS sea-level hindcast. Additionally, locations of the tide gauges where hindcast validation with in-situ measurements is performed are depicted.	15
2	4-month comparison of the HIPOCAS hindcast RSS (solid line) with in situ observation (plus mark) (in m) at BARC.	16
3	Spatial distribution of time correlations between tide gauge observations and HIPOCAS hindcasted data for RSS.	17
4	9-year time series of monthly mean RSS (in cm) from HIPOCAS hindcast (solid line) and from in-situ measurements at VIGO (plus marks).	18
5	5-year comparison of satellite inferred RSS data (plus marks) with that obtained through the HIPOCAS simulation (solid line) around the BARC station.	19
6	Spatial distribution of the long-term mean of HIPOCAS hindcasted RSS (in cm).	20
7	Spatial distribution of a 44-year (1958-2001) average of monthly mean sea level pressure obtained from the HIPOCAS atmospheric hindcast.	21
8	Spatial distribution of the maximum RSS (in cm) obtained from the whole 44-year HIPOCAS hindcast. Note that the maximum may not take place at the same time for each grid point of the spatial domain.	22
9	Annual variation of different percentiles for RSS (in cm) obtained from the HIPOCAS hindcast at a location in the Gulf of Lyon (4.0E, 42.5N). Similar symbols are used for top and bottom percentile values, being used the + symbol for maximum (percentile 100th) and minimum (percentile 0th), open diamond for percentile 99th and 1st, open triangle for percentile 90th and 10th, and open square for percentile 50th.	23
10	Spatial distribution of (a) long-term RSS change rates (mm/yr), and (b) long-term change rates for RSS extreme values (represented by the percentile 99th, in mm/yr). Data are derived from the whole 44-year HIPOCAS hindcast.	24

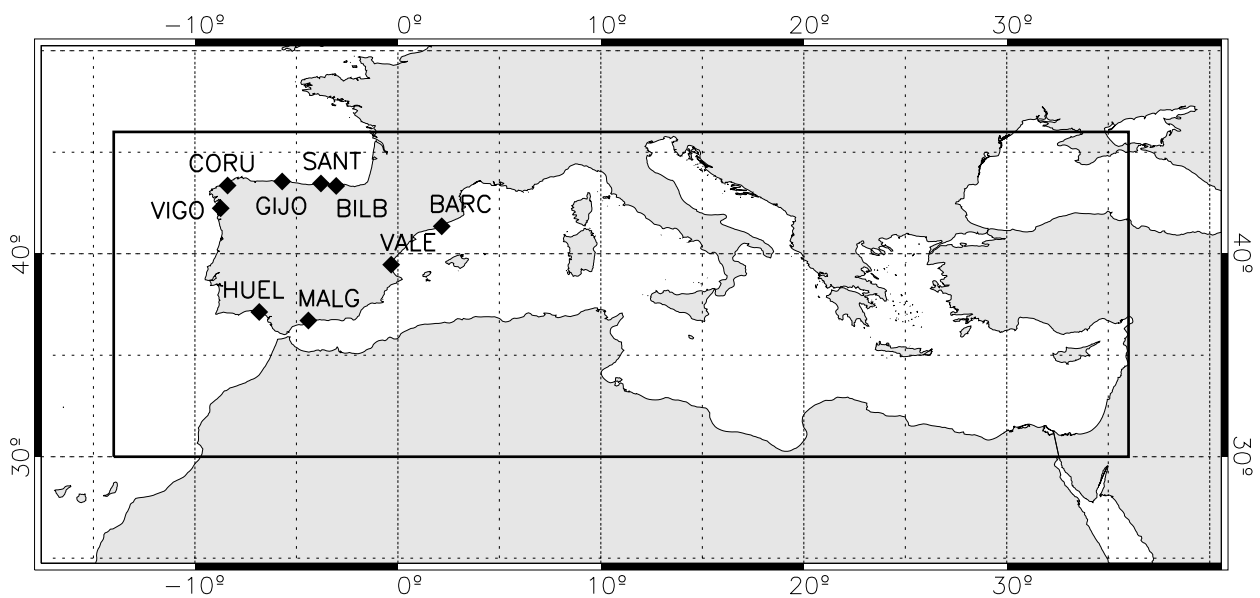


Figure 1: Spatial domain covered by the HIPOCAS sea-level hindcast. Additionally, locations of the tide gauges where hindcast validation with in-situ measurements is performed are depicted.

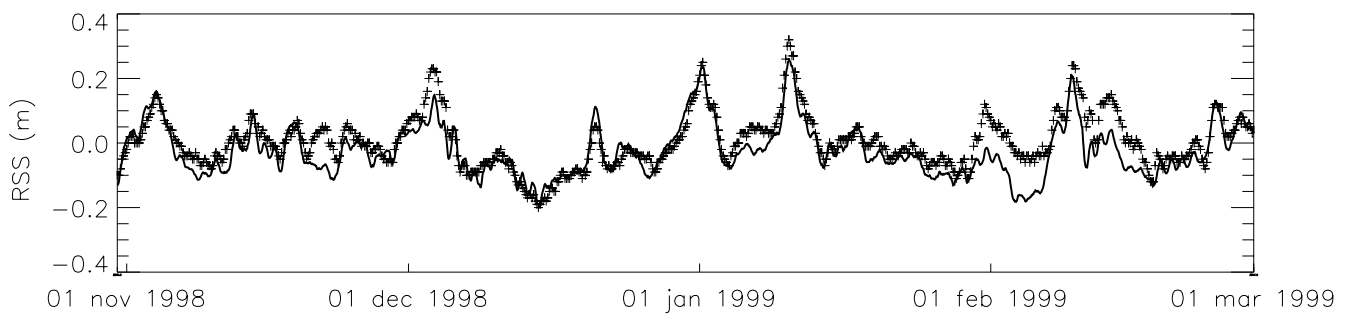


Figure 2: 4-month comparison of the HIPOCAS hindcast RSS (solid line) with in situ observation (plus mark) (in m) at BARC.

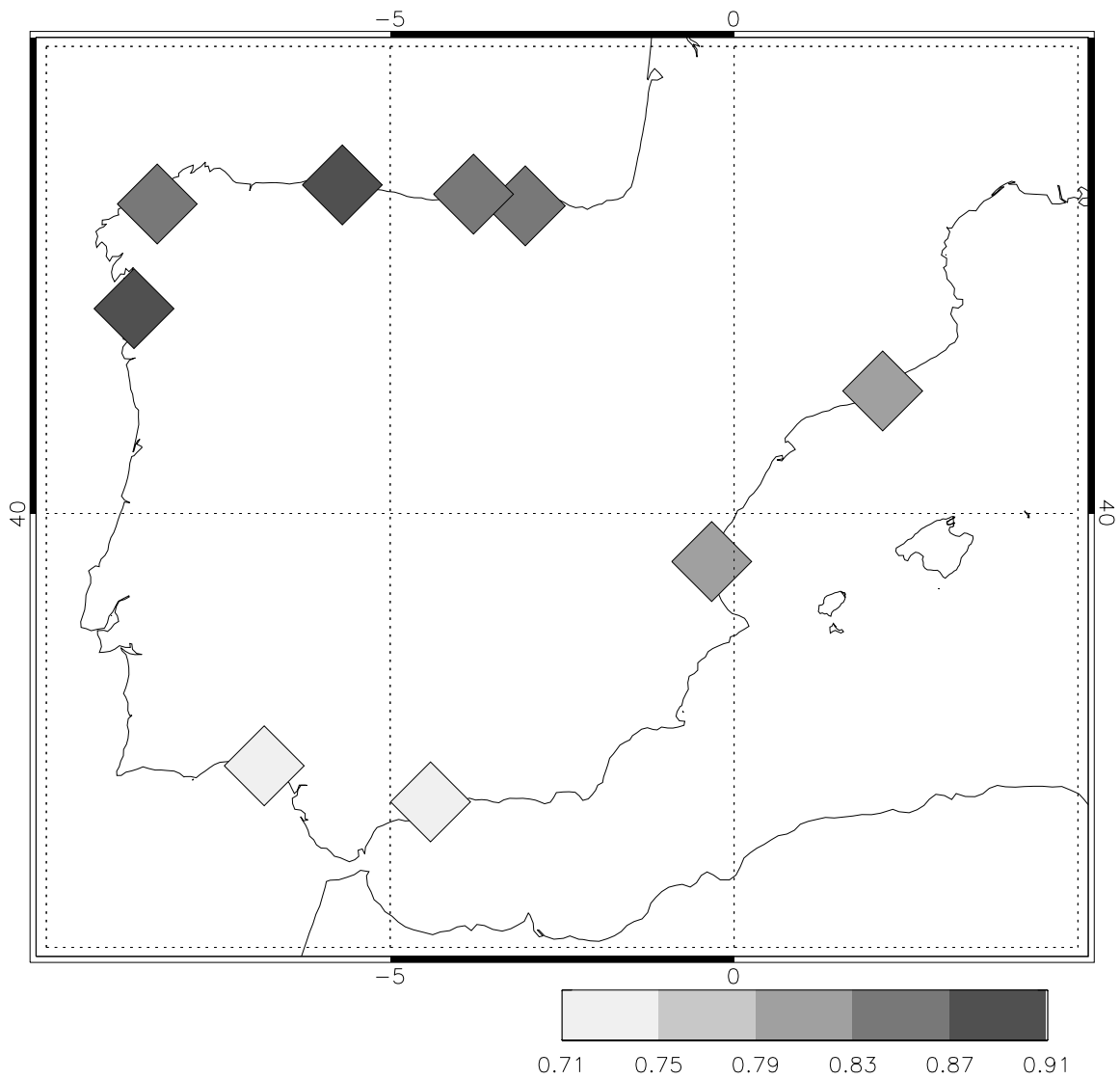


Figure 3: Spatial distribution of time correlations between tide gauge observations and HIPOCAS hindcasted data for RSS.

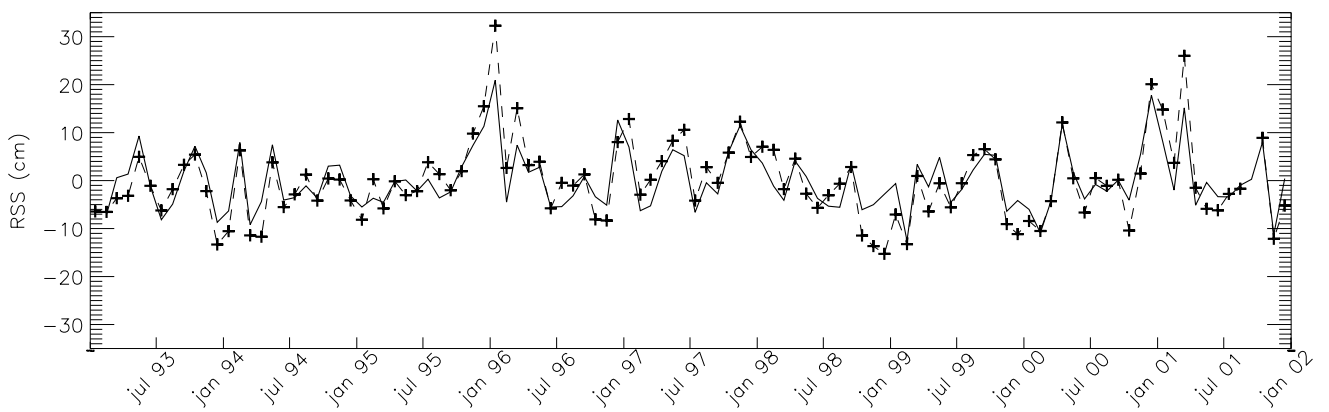


Figure 4: 9-year time series of monthly mean RSS (in cm) from HIPOCAS hindcast (solid line) and from in-situ measurements at VIGO (plus marks).

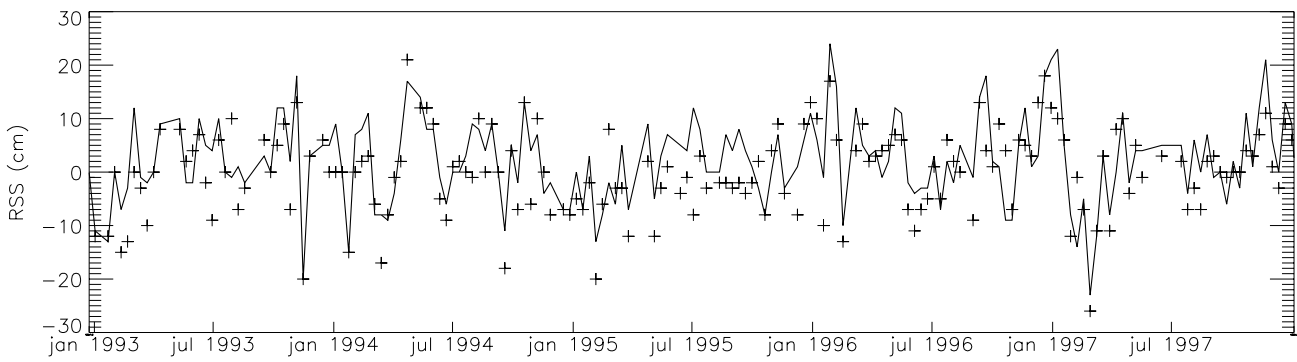


Figure 5: 5-year comparison of satellite inferred RSS data (plus marks) with that obtained through the HIPOCAS simulation (solid line) around the BARC station.

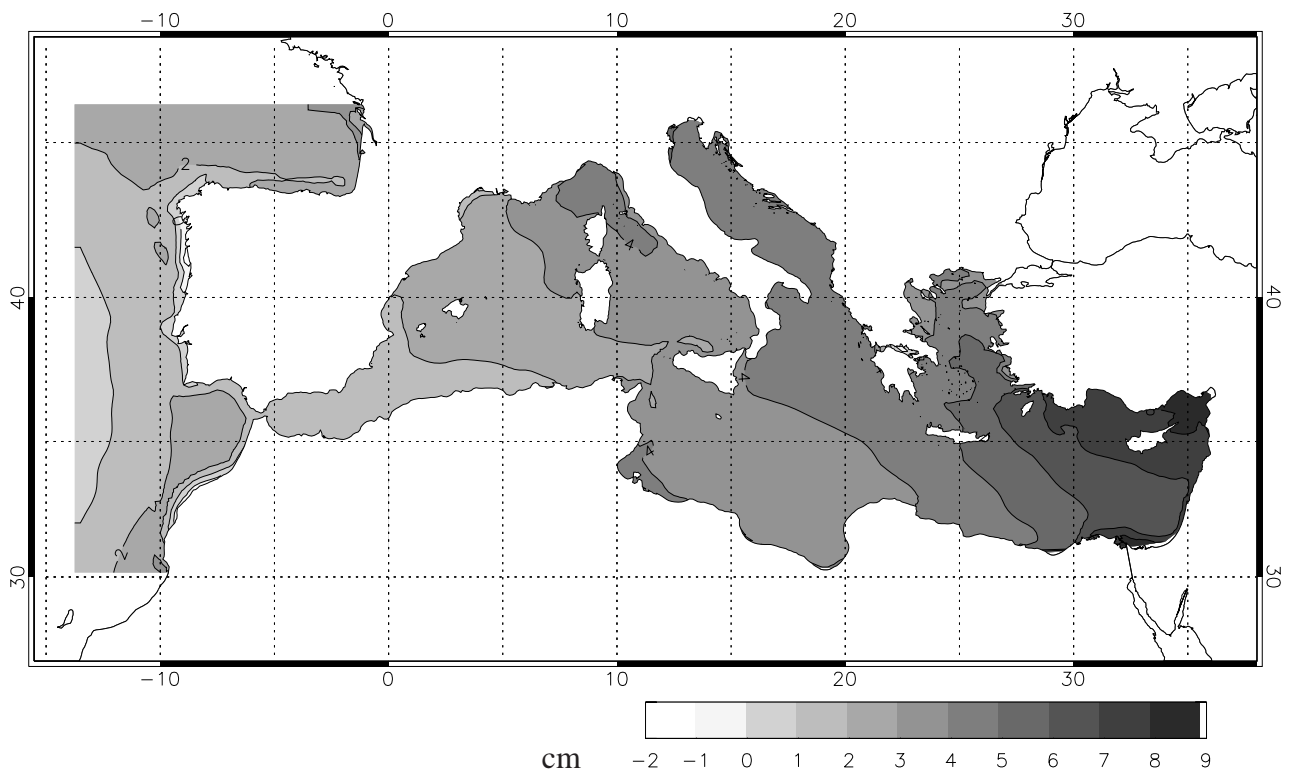


Figure 6: Spatial distribution of the long-term mean of HIPOCAS hindcasted RSS (in cm).

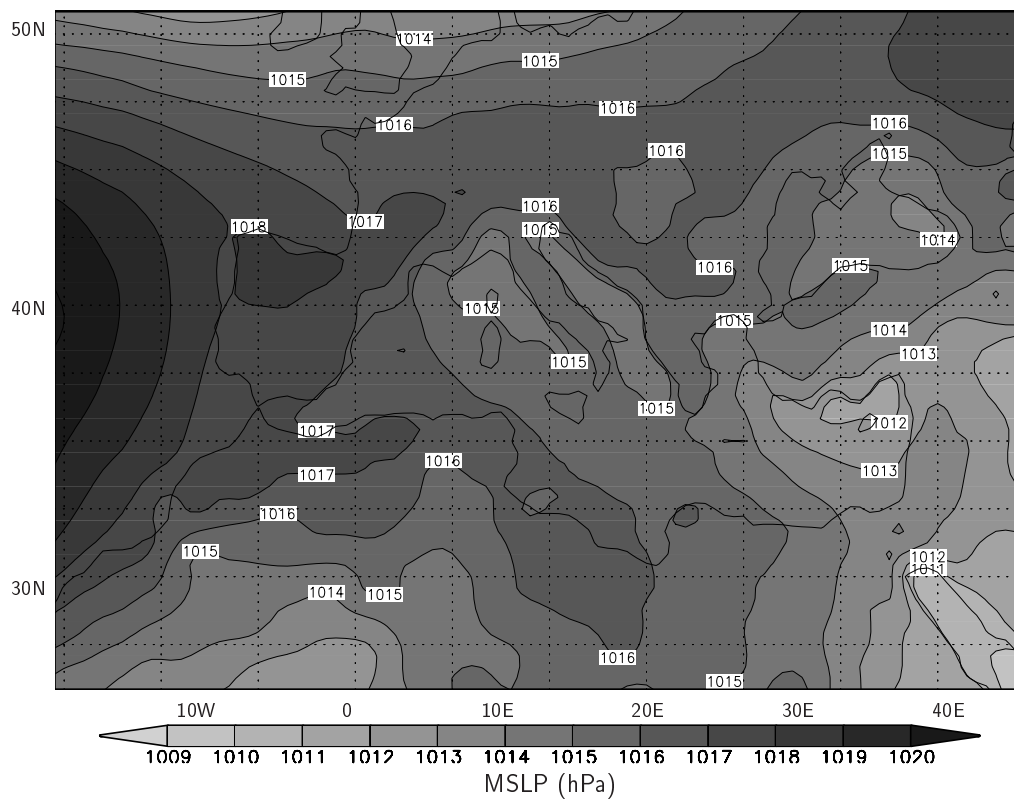


Figure 7: Spatial distribution of a 44-year (1958-2001) average of monthly mean sea level pressure obtained from the HIPOCAS atmospheric hindcast.

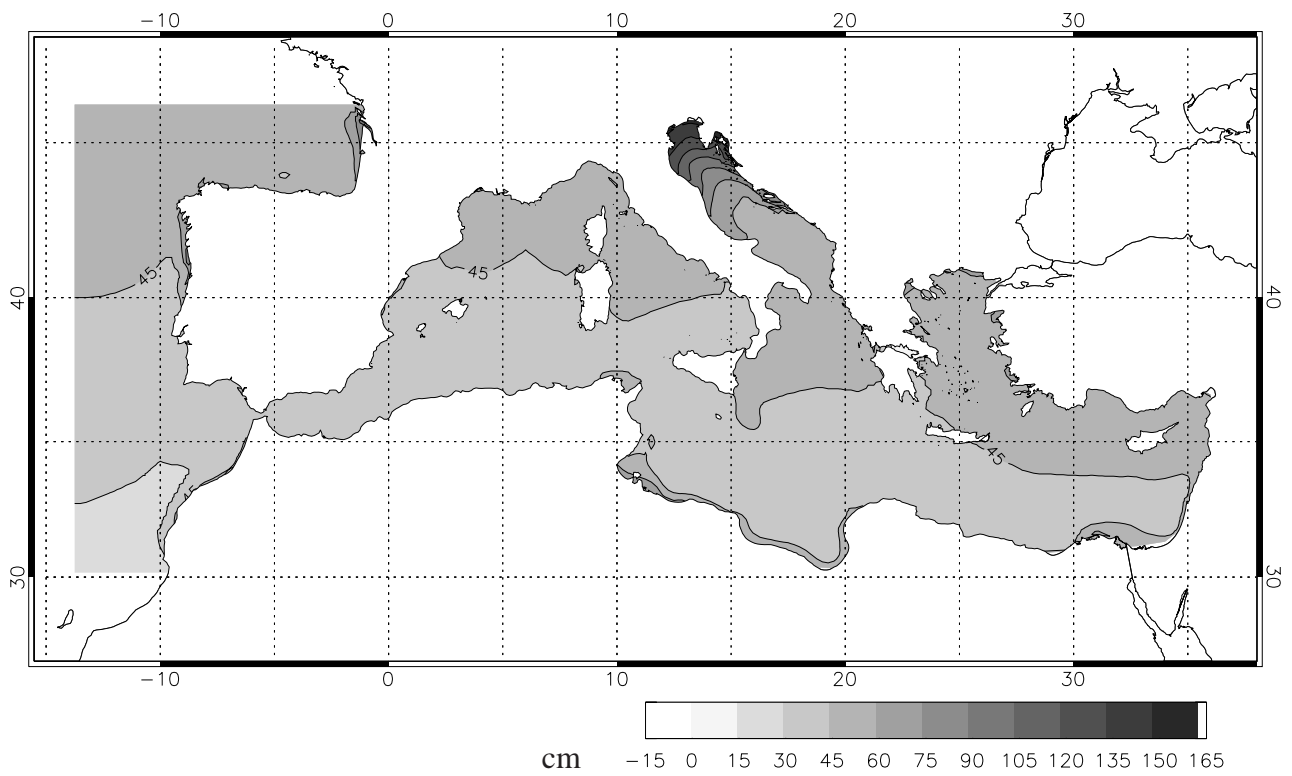


Figure 8: Spatial distribution of the maximum RSS (in cm) obtained from the whole 44-year HIPOCAS hindcast. Note that the maximum may not take place at the same time for each grid point of the spatial domain.

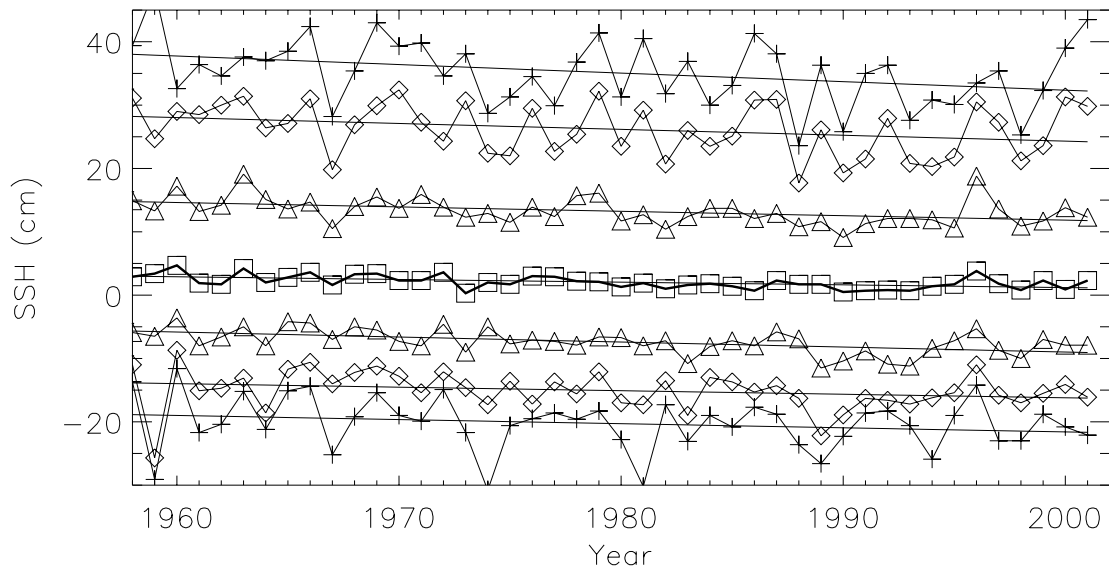


Figure 9: Annual variation of different percentiles for RSS (in cm) obtained from the HIPOCAS hindcast at a location in the Gulf of Lyon (4.0E, 42.5N). Similar symbols are used for top and bottom percentile values, being used the + symbol for maximum (percentile 100th) and minimum (percentile 0th), open diamond for percentile 99th and 1st, open triangle for percentile 90th and 10th, and open square for percentile 50th.

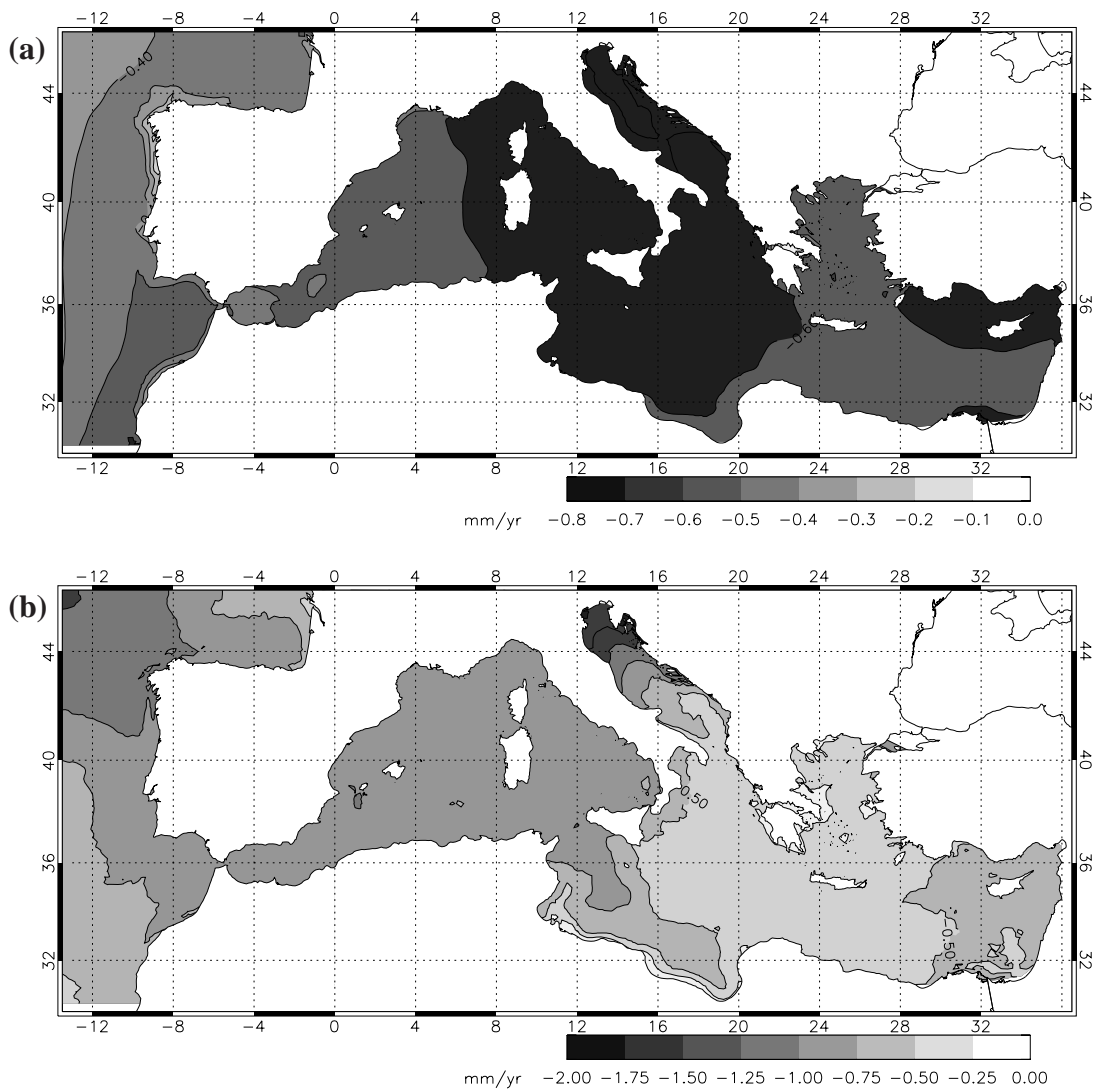


Figure 10: Spatial distribution of (a) long-term RSS change rates (mm/yr), and (b) long-term change rates for RSS extreme values (represented by the percentile 99th, in mm/yr). Data are derived from the whole 44-year HIPOCAS hindcast.

List of Tables

- 1 General statistics derived from the comparison between tide gauge and model HIPOCAS data. **r** is stands for correlation index, **RMSE** for root mean square error, **bias** for differences hindcast minus in-situ, and **n** for the number of data used in the statistics. 26
- 2 Statistical comparison of the RSS obtained from the HIPOCAS hindcast (subscript *h*) with that inferred from Topex-Poseidon (subscript *s*). Period of comparison is 1992-2001. **n**: Number of collocated data, **r**: correlation index, **RMSE**: root mean square error, \bar{X} : mean RSS, **Std**: standard deviation, **bias**: hindcast minus satellite data. 27

Tide gauges	r	RMSE	bias	n
BILB (3.04W, 43.34N)	0.86	5.60	-1.98	77438
SANT (3.78W, 43.46N)	0.85	5.79	-2.16	78569
GIJO (5.70W, 43.56N)	0.87	5.77	-3.62	48835
CORU (8.39W, 43.36N)	0.84	6.48	-0.66	59232
VIGO (8.73W, 42.24N)	0.88	6.06	0.23	75219
HUEL (6.83W, 37.13N)	0.74	6.60	-0.52	42494
MALG (4.41W, 36.71N)	0.71	5.94	-0.76	75903
VALE (0.33W, 39.46N)	0.81	5.43	-1.71	71982
BARC (2.16E, 41.35N)	0.82	5.26	4.24	74357

Table 1: General statistics derived from the comparison between tide gauge and model HIPOCAS data. **r** is stands for correlation index, **RMSE** for root mean square error, **bias** for differences hindcast minus in-situ, and **n** for the number of data used in the statistics.

Name	n	r	RMSE	\bar{X}_s	Std_s	Std_h	bias
BILB	329	0.74	6.7	1.7	8.7	9.4	-1.7
CORU	331	0.83	6.2	1.3	10.5	10.4	-1.3
MALG	293	0.68	6.3	1.0	6.2	8.5	-1.0
VALE	322	0.79	5.5	1.5	7.8	8.4	-1.3
BARC	307	0.80	5.9	2.3	8.4	8.5	-2.3

Table 2: Statistical comparison of the RSS obtained from the HIPOCAS hindcast (subscript h) with that inferred from Topex-Poseidon (subscript s). Period of comparison is 1992-2001. n : Number of collocated data, r : correlation index, **RMSE**: root mean square error, \bar{X} : mean RSS, **Std**: standard deviation, **bias**: hindcast minus satellite data.